Trials on Tissue Contractility Estimation from Cardiac Cine MRI Using a Biomechanical Heart Model

R. Chabiniok[1], P. Moireau[1], P.-F. Lesault[2], A. Rahmouni[2], J.-F. Deux[2], and D. Chapelle[1]

[1] INRIA, MACS Team, B.P. 105, 78153 Le Chesnay, France
[2] AP-HP Hôpital Henri Mondor, Université Paris-Est Créteil, France

Abstract. In this paper we apply specific data assimilation methods in order to estimate regional contractility parameters in a biomechanical heart model, using as measurements *real* Cine MR images obtained in an animal experiment. We assess the effectiveness of this estimation based on independent knowledge of the controlled infarcted condition, and on late enhancement images. Moreover, we show that the estimated contractility values can improve the model behavior in itself, and that they can serve as an indicator of the local heart function, namely, to assist medical diagnosis for the post-infarct detection of hypokinetic or akinetic regions in the myocardial tissue.

1 Introduction

Building adequate *patient-specific* models is now widely recognized as a most important challenge for bioengineering applied in medicine, and this holds in particular for cardiac modeling [18]. Of course, as a first major ingredient, this requires the construction of accurate *anatomical* models which suitably represent the actual geometrical attributes of the patient considered, usually based on medical imaging data. The next – at least equally important, and particularly challenging – stage consists in "personalizing" the biophysical characteristics of a cardiac model in order to reproduce the specificities of the patient, as e.g. in case of various pathologies which are likely to perturb localized values of constitutive parameters. This step is crucial to render the model *predictive*, hence to obtain some clinically-relevant quantitative information from the model simulations, both in the current state of the patient and under various scenarii of future evolutions, such as for therapy planning.

The complexity of the heart physiology – and of the related models – is such that this biophysical personalization procedure cannot be simply performed "manually", such as by directly extracting the required quantities from the available measurements, hence some automated estimation procedures are much needed in this endeavor [1]. Moreover, as some biophysical parameters are strongly correlated with the functional state of the organ, the automatic estimation of these parameters can be envisioned as a diagnosis tool. Our approach corresponds to the concept of *data assimilation* – already widely employed in other

D.N. Metaxas and L. Axel (Eds.): FIMH 2011, LNCS 6666, pp. 304–312, 2011.

domains of science and engineering – notably different from the objective of cardiac motion tracking *per se* [15,10,2,17], sometimes complemented by extracting some valuable indices from available data by using some constraining physical model equations [7,9]. The discriminating criterion in data assimilation is that once the estimation has been performed the biophysical model must be able to run *independently of any data*, while providing accurate and *predictive* solutions.

In this paper, we will consider a biomechanical heart model as proposed in [16] and perform a *complete personalization* – namely, both anatomical and biophysical – using *actual clinical data* consisting of Cine MR image sequences and pressure measurements, based on some earlier-proposed estimation procedures [12,13,11]. In order to allow for a detailed assessment of the estimation results, we used data obtained in an animal experiment in which a controlled infarct was created [4]. Hence, we can quantitatively compare the estimation results pertaining to the main biophysical parameter of interest in this context – namely, the tissue contractility – obtained prior and after infarction, and also qualitatively and semi-quantitatively evaluate the post-infarct results with respect to *a priori* knowledge regarding the pathology and to late enhancement indicators.

The next section will be devoted to the description of experimental data and an overview of the biomechanical model considered. Then, in Section 3 we summarize the estimation methodology and present the personalization results. A discussion follows in Section 4, prior to concluding remarks.

2 Experimental Data and Direct Modeling

The animal experiment including the data acquisition and setup of the direct model was described in [4]. Here, we will summarize the experimental data acquisition and the calibration strategy for the healthy and the infarcted hearts.

2.1 Experimental Data

The experimental data consist of animal data obtained with a farm pig of 30 kg. The subject was examined and data acquired once in a baseline condition (physiological heartbeat), and 38 days after artificially creating an antero-septal infarct. In both stages, non-invasive MR image data – among which Cine MRI and late enhancement images were used to set up the models – were acquired, and pressures in the heart cavities and large vessels were measured by catheterization.

2.2 Anatomical Model

Anatomical models for the baseline and infarcted stage were created from the end-diastolic time frames of the Cardiac MR images. We emphasize that two different anatomical models had to be created, in particular due to significant anatomical changes (thinning of the post-infarcted LV wall caused by resorption of the necrosis and tissue remodeling). Fiber directions were defined using prescribed values of angles between the short axis plane and the fibers on the

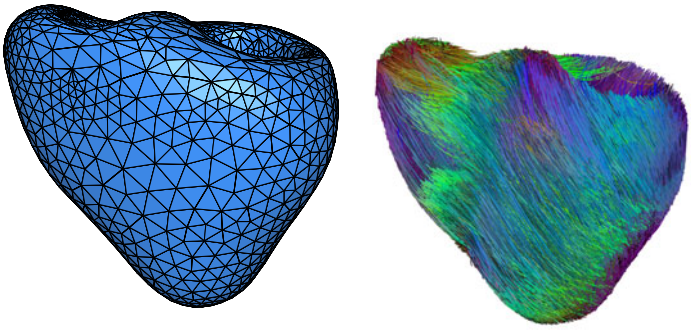

Fig. 1. Computational mesh for baseline (left) and generic fibers prescribed in the mesh (right)

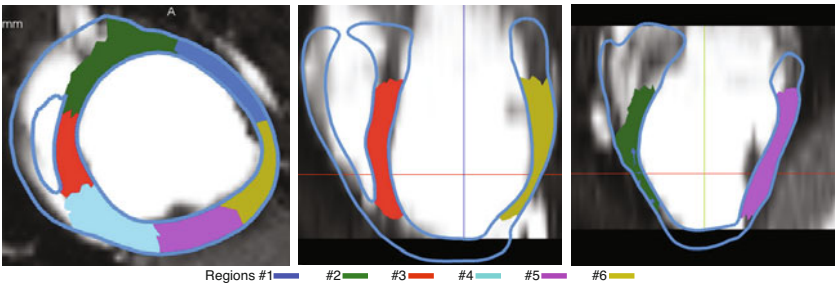

Fig. 2. Mesh of T0+38 subdivided into 6 volumic regions in the left ventricle

epicardium and endocardium, namely, -60/60 degrees in the LV, and -50/50 degrees in the RV, see Figure 1. The left ventricle of each model was subdivided into 6 volume regions – corresponding in their upper third to the basal segments of the standard 17-segment LV subdivision proposed by the American Heart Association (AHA) in [3], see Figure 2 – in order to allow prescribing and estimating different values of physical parameters in each region, in particular to characterize the infarct. In addition, for assessment purposes the non-viable tissue in the infarcted stage was segmented from the late enhancement images and projected into the corresponding model, see Fig. 3.

2.3 Biophysical Model

The cardiac model considered was described in [16], see also [6] for a more complete physiological and physical substantiation. In this model, a prescribed electrical activation induces actin-myosin binding, hence an active stress along the fiber direction. It has already been demonstrated in [4] that the main effects of an infarct can be captured in this model by reducing the contractility parameter which relates the electrical activation to the mechanical quantities.

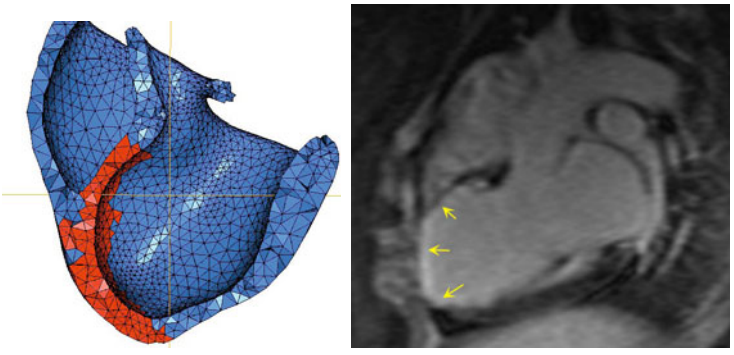

Fig. 3. Infarcted tissue in the mesh (left, in red) as segmented from the late enhancement MR images (right, yellow arrows)

The setup of the direct model of the healthy stage follows the calibration procedure used in [5]. The main mechanical parameters of the model – namely, the active properties represented by the contractility, and the passive tissue stiffness parameters – were adjusted manually. These parameters were kept constant over the whole myocardium. We used visco-elastic boundary conditions ([14]) applied on the base of the ventricles (area around the valves) and in the area around the apex, with parameters adjusted to obtain a still apex while preserving the base motion as seen in the long axis Cine MR images. An additional visco-elastic boundary condition representing a contact between the anterior heart wall with the thoracic cage was used. Finally, the Windkessel models parameters were adjusted so as to obtain simulated ventricle and arterial pressures close to the measured values.

In all our simulations we used an analytically prescribed electrical activation pattern in which a planar wave propagates from the apex to the base while activating only the subendocardial part of the myocardium. The transmural propagation is represented by a traveling wave with a lower propagation velocity. The two velocities are adjusted in the baseline case so that the activation timing is physiological, namely: propagation along the endocardium in ∼30–35 ms; endo- to epicardium propagation in ∼30–35 ms; activation of the whole myocardium in ∼70–80 ms, which corresponds to the measured QRS duration. The action potential duration in the simulation was taken constant over the whole myocardium, and was adjusted according to the Cine MRI data.

3 Regional Contractility Estimation Using Data Assimilation

3.1 Data Assimilation Methodology

Data assimilation consists in using measurements available on the system considered in order to estimate the state variables – namely, the actual trajectory

taken by the real system – and some unknown or uncertain modeling parameters. In this study we employed a sequential type data assimilation procedure – also referred to as filtering – by which the model dynamics and the uncertain parameters are corrected all along the simulation window using an operator which characterizes the *discrepancy* between the current simulated state and the measurements [12,8]. A successful procedure allows to achieve rapid convergence of the simulated trajectory to the real one and of the parameter quantities to their actual values. Furthermore, the essential physical behavior of the model is not perturbed, hence once the actual state and parameters have been recovered the model can be considered to be adequately *personalized*. The model can then be used to obtain information on some biophysical quantities absent from the measurements, or to predict the evolutions of the system under various assumptions, such as to explore and assess therapeutic strategies.

3.2 Estimation Using Segmented Cine MRI

In our case we will use the segmented Cine MRI sequences to construct a discrepancy operator based on the distance maps of the model boundary to the segmentation contours, separately on the LV endo- and epicardium. This discrepancy is employed in a filtering approach named "Schur Displacement Feedback" (SDF) which provides an effective state estimator as discussed in [13,8]. In addition, parameter estimation is performed by incorporating a second-stage filter which corresponds to a reduced-order version of the "Unscented Kalman Filter" (UKF), see [11]. This method generalizes reduced-order Kalman filtering to nonlinear dynamical and discrepancy operators – and indeed would be equivalent for linear systems – without requiring the computation of tangent operators and with enhanced accuracy compared to Extended Kalman Filtering.

We used this joint state-parameter estimation approach to estimate both the trajectory and regionalized contractility values – scaled to one according to a nominal healthy value – in each of the 6 above-described regions. As regards the estimation procedure setup, 3 main parameters had to be adjusted, namely, the covariance of the (scaled) contractility parameters set to $1/7$, the standard deviation of the observation error corresponding to roughly 1.5 mm in the segmentation, and the gain of the SDF filter manually calibrated to maintain the simulated system "reasonably close" to the data.

3.3 Estimation Results

Figure 4 shows the regional contractility estimation results, both in the baseline and in the infarcted stages. We emphasize that – by construction of the filtering procedure – the estimated parameter values evolve during the simulation period – corresponding to a complete heartbeat in our case – and of course the actual estimation is achieved with the final values. Note that these estimation curves actually stabilize near the end of the simulation window.

We also show in Figure 5 a comparison of the Cine MRI at the infarcted stage with three model contours: a direct simulation without estimation and with nominal contractility parameter values; the joint state-parameter estimator; finally,

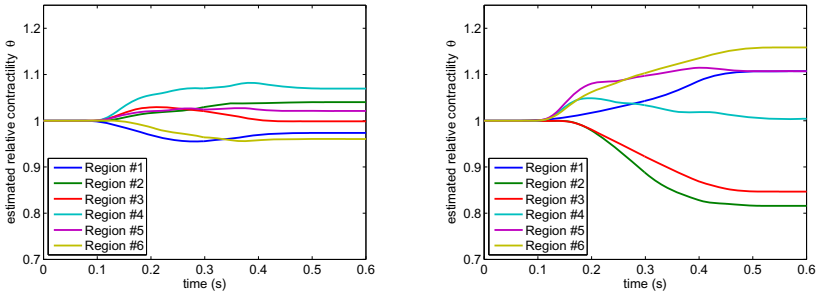

(a) Baseline (b) T0+38

Fig. 4. Regional contractility estimation at each stage

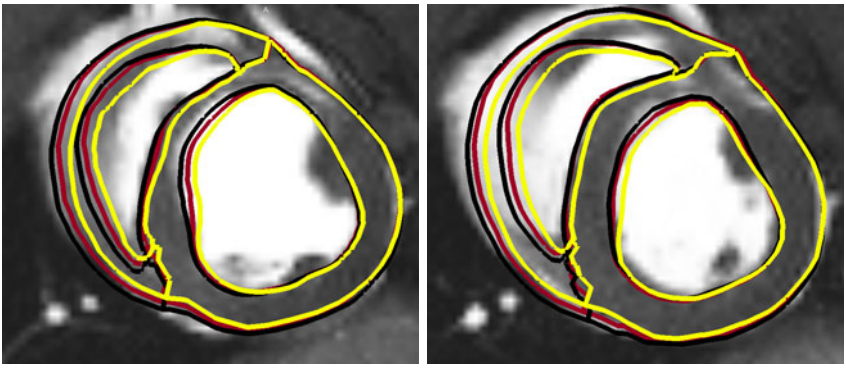

Fig. 5. Two slices of the end-systolic phase at stage T0+38. Comparison of direct model with constant contractility (yellow contour), direct model using the estimated values of contractility (red), joint state-parameter estimation (black).

a direct simulation without estimation and with the contractility parameter values obtained in the estimation procedure. We can see that – as expected – the estimator is closest to the image contours, but the direct simulation with personalized parameters is also quite accurate, and in particular drastically reduces the thickening in the infarcted region, unlike in the nominal simulation.

We can also assess the estimation results by comparison with the proportion of tissue marked by the late enhancement in each region. The plot shown in Figure 6 displays a good correlation between these computed ratios $(r_i)_{i=1}^6$ and the corresponding values obtained from the estimated contractility parameters $(\theta_i)_{i=1}^6$ by assuming the simple interpolation rule $\theta_i = 0.25 r_i + 1.20(1 - r_i)$. Of course, it should be noted that the segmentation of late enhancement images can be expected to be affected by various errors, hence it does not provide any definite "ground truth".

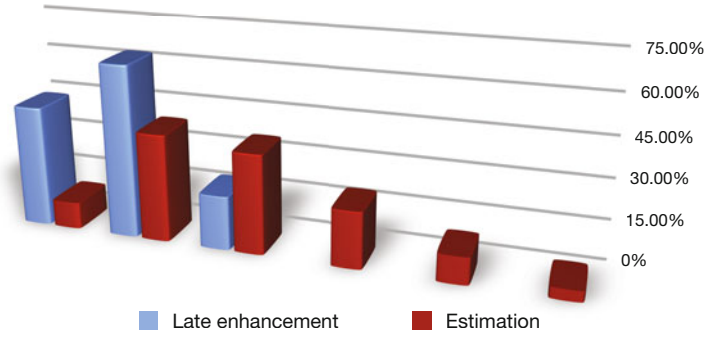

Fig. 6. Relative extent of the infarct in each region computed from the late enhancement segmentation and inferred from the estimated parameters (regions ordered from left to right)

4 Discussion

As seen in Figure 4, in the baseline case the contractility values do not vary more than by 10% in the course of the estimation. At the infarcted stage, a pronounced drop of contractility in the infarcted regions – except for Region ♯1 – is obtained, together with an increase in Regions ♯5 and ♯6 which may be caused by a compensation hypertrophy.

The contractility overestimation in the anterior wall at the infarcted stage (Region ♯1) may be caused by the artificial boundary conditions applied on the adjacent epicardial surface. The prescription and adjustment of suitable boundary conditions is a difficult problem, as we need to represent the contact of the heart with the surrounding structures – mainly the thoracic cage and the diaphragm – for which we used visco-elastic boundary conditions. However, this type of boundary condition applied on the anterior wall (part of Region ♯1) clearly hinders contraction. The hypokinesis of the region is then corrected by the parameter estimation, inducing an increase of the estimated contractility parameter in Region ♯1, see Figure 4. For this reason mainly related to a modeling limitation, we introduce some error in the parameter estimation for Region ♯1. This modeling issue may be circumvented by considering a sliding boundary condition on the anterior wall – much more realistic than the tethering associated with viscoelastic support, indeed – but such boundary conditions are quite delicate to handle and require very smooth surface meshes to allow adequate sliding.

Nevertheless, considering the relative coarseness of the measurements used in the estimation procedure – namely, only two segmented surfaces in each snapshot, the results obtained for the regional contractility values are undoubtedly satisfactory, as also substantiated by the personalized simulation produced with these estimated values, recall Fig. 5.

5 Conclusion and Perspectives

In this paper, we successfully applied a methodology of sequential joint-state parameter estimation with real cardiac Cine MRI data. As a result, this approach provides an automatic biophysical personalization of the model, which enables further uses for predictive purposes with key perspectives in therapy planning. Furthermore, we were able to localize and quantify myocardial infarction via regional contractility parameters, which shows some valuable potential for diagnosis assistance.

Of course, with a view to diagnosis assistance, more detailed regional contractility maps – e.g. a 17-segment AHA subdivision of the left ventricle, possibly further subdivided into several layers – would be extremely valuable. Our results indicate that observability conditions intrinsically limit the information which can be extracted from mere segmented Cine sequences. However, we could also employ tagged MR images, either with directly extracted myocardium displacements, or by extending in a straightforward manner the estimator used in this work based on measuring distances between the simulated and observed surfaces with the tag planes [8]. We can conjecture that the level of details accessible with this type of data would be significantly enhanced, and we could also expect to benefit from this to estimate some other physical parameters, such as passive tissue stiffness or quantities pertaining to the electrical activation.

References

1. Augenstein, K.F., Cowan, B.R., LeGrice, I.J., Nielsen, P.M.F., Young, A.A.: Method and apparatus for soft tissue material parameter estimation using tissue tagged magnetic resonance imaging. J. Biomech. Eng. 127(1), 148–157 (2005)
2. Bogatyrenko, E., Hanebeck, U.: Simultaneous state and parameter estimation for physics-based tracking of heart surface motion. In: Multisensor Fusion and Integration for Intelligent Systems (MFI), pp. 109–114 (2010)
3. Cerqueira, M.D., et al.: Standardized myocardial segmentation and nomenclature for tomographic imaging of the heart: A statement of healthcare professionals from the cardiac imaging comittee of the Council on Clinical Cardiology of the American Heart Association. Circulation 105, 539–542 (2002)
4. Chabiniok, R., Chapelle, D., Lesault, P.-F., Rahmouni, A., Deux, J.-F.: Validation of a biomechanical heart model using animal data with acute myocardial infarction. In: Proc. of CI2BM 2009 - MICCAI Workshop (2009)
5. Chapelle, D., Fernández, M.A., Gerbeau, J.-F., Moireau, P., Sainte-Marie, J., Zemzemi, N.: Numerical simulation of the electromechanical activity of the heart. In: Ayache, N., Delingette, H., Sermesant, M. (eds.) FIMH 2009. LNCS, vol. 5528, pp. 357–365. Springer, Heidelberg (2009)
6. Chapelle, D., Le Tallec, P., Moireau, P., Sorine, M.: An energy-preserving muscle tissue model: formulation and compatible discretizations. Int. J. Multiscale Comput. Eng. (2011) (in press)
7. Hu, Z.H., Metaxas, D., Axel, L.: In vivo strain and stress estimation of the heart left and right ventricles from MRI images. Med. Image Anal. 7(4), 435–444 (2003)

8. Imperiale, A., Chabiniok, R., Moireau, P., Chapelle, D.: Constitutive parameter estimation methodology using tagged-MRI data. In: Metaxas, D.N., Axel, L. (eds.) FIMH 2011. LNCS, vol. 6666, pp. 409–417. Springer, Heidelberg (2011)
9. Liu, H., Shi, P.: Maximum a posteriori strategy for the simultaneous motion and material property estimation of the heart. IEEE Trans. Biomed. Eng. 56(2), 378–389 (2009)
10. Mansi, T., Peyrat, J.-M., Sermesant, M., Delingette, H., Blanc, J., Boudjemline, Y., Ayache, N.: Physically-constrained diffeomorphic demons for the estimation of 3D myocardium strain from cine-MRI. In: Ayache, N., Delingette, H., Sermesant, M. (eds.) FIMH 2009. LNCS, vol. 5528, pp. 201–210. Springer, Heidelberg (2009)
11. Moireau, P., Chapelle, D.: Reduced-order Unscented Kalman Filtering with application to parameter identification in large-dimensional systems. Cont. Optim. and Calc. Variat. (2010)
12. Moireau, P., Chapelle, D., Le Tallec, P.: Joint state and parameter estimation for distributed mechanical systems. Comput. Meth. Appl. Mech. Eng. 197, 659–677 (2008)
13. Moireau, P., Chapelle, D., Le Tallec, P.: Filtering for distributed mechanical systems using position measurements: Perspectives in medical imaging. Inverse Prob. 25(3), 035010 (2009)
14. Moireau, P., Xiao, N., Astorino, M., Figueroa, C.A., Chapelle, D., Taylor, C.A., Gerbeau, J.-F.: External tissue support and fluid-structure simulation in blood flows. Biomech. Model. Mechanobiol. (2011) (in press)
15. Papademetris, X., Sinusas, A.J., Dione, D.P., Constable, R.T., Duncan, J.S.: Estimation of 3D left ventricular deformation from medical images using biomechanical models. IEEE Trans. Med. Imaging 21(7), 786–800 (2002)
16. Sainte-Marie, J., Chapelle, D., Cimrman, R., Sorine, M.: Modeling and estimation of the cardiac electromechanical activity. Comput. Struct. 84, 1743–1759 (2006)
17. Schaerer, J., Casta, C., Pousin, J., Clarysse, P.: A dynamic elastic model for segmentation and tracking of the heart in MR image sequences. Med. Image Anal. 14, 738–749 (2010)
18. Sermesant, M., Moireau, P., Camara, O., Sainte-Marie, J., Andriantsimiavona, R., Cimrman, R., Hill, D.L., Chapelle, D., Razavi, R.: Cardiac function estimation from MRI using a heart model and data assimilation: advances and difficulties. Med. Image Anal. 10(4), 642–656 (2006)